Journal of Organometallic Chemistry 694 (2009) 2700–2704

Contents lists available at ScienceDirect

Journal of Organometallic Chemistry

journal homepage: www.elsevier.com/locate/jorganchem

Effect of ancillary ligands on the properties of heteroleptic green iridium dendrimers functionalized with carbazole dendrons

Junqiao Ding, Jianhong Lü, Yanxiang Cheng, Zhiyuan Xie, Lixiang Wang *, Xiabin Jing, Fosong Wang

State Key Laboratory of Polymer Physics and Chemistry, Changchun Institute of Applied Chemistry, Chinese Academy of Sciences, Changchun 130022, PR China

ARTICLE INFO

Article history:
Received 12 January 2009
Received in revised form 24 March 2009
Accepted 24 March 2009
Available online 2 April 2009

Keywords:
Iridium
Homoleptic dendrimer
Heteroleptic dendrimer
Non-doped device

ABSTRACT

A series of heteroleptic green iridium dendrimers functionalized with carbazole dendrons, such as **G2(pic)** and **G2(acac)**, have been synthesized, in which picolinic acid and acetylacetone are used as the ancillary ligands, respectively. Compared with the corresponding homoleptic iridium dendrimer **G2** (8%), these heteroleptic ones can be prepared under mild conditions with total yields as high as 55–67%. Both the dendrimer **G2(pic)** and **G2(acac)** display bright green emissions with photoluminescence quantum yields higher than 0.80 in toluene solution. As a result, a maximum external quantum efficiency of 7.1% (21.0 cd/A) for **G2(pic)** and 7.7% (25.8 cd/A) for **G2(acac)** has been realized based on non-doped device configuration. The state-of-art performance indicates that the heteroleptic dendrimers can be promising candidates used for non-doped electrophosphorescent devices, especially when the ease of synthesis in a large scale is considered.

1. Introduction

Dendrimers are of great importance for their application in optoelectronic devices since they possess the advantages of both the well-defined structures of small molecules and the solution processibility of polymers [1,2]. Due to their inherent topological features, phosphorescent iridium (Ir) dendrimers have been developed, in which an Ir complex is surrounded by a branched shell to prevent self-aggregation or concentration quenching of emissive core in the solid state. By use of this steric protection, Burn et al. first reported phenylene-dendronized Ir dendrimers [3–5]. However, poor charge transport capability of phenylene dendrons significantly limited electroluminescence (EL) performance of these materials. Thus, to achieve better charge transport, triphenylamines were introduced as dendrons because of their ability to transport positive charge via their radical cations. However, the efficiency decayed sharply with increasing dopant concentration and excimer appeared at high dopant concentration [6]. In order to realize highly efficient non-doped electrophosphorescent devices, oligocarbazole-based dendrons with host function were introduced into Ir complexes [7].

Although functional metallophosphors [8,9] for effective charge carrier injection/transport have been actively investigated recently by introducing carbazole units into the transition-metal-based complexes [10–14], little attention has been paid to their host function aiming to develop non-doped phosphorescent materials. With this idea in mind, efficient homoleptic green Ir dendrimers have been successfully designed and prepared. With our expectation, the efficiency of non-doped device was as high as 34.7 cd/A for the second generation dendrimer **G2**. However, the synthesis of homoleptic Ir dendrimers needed high temperature and the yields were very low [15], especially for high generation dendrimers. For example, only 8% yield for **G2** was obtained [7]. In contrast, according to the literature [16], the heteroleptic ones were easy to be synthesized under mild conditions with high yields.

On the consideration of large scale preparation, herein a series of heteroleptic green Ir dendrimers, such as **G2(pic)** and **G2(acac)**, have been synthesized and characterized, in which picolinic acid (Hpic) and acetylacetone (Hacac) were used as the ancillary ligands, respectively. Although heteroleptic Ir dendrimers have been reported before [17,18], the difference between homoleptic and heteroleptic Ir dendrimers was rarely investigated. Therefore, in this article the effect of ancillary ligands on the photophysical properties and non-doped device performance of the Ir dendrimers was researched in detail.

2. Results and discussion

As illustrated in Scheme 1, the synthesis of heteroleptic Ir dendrimers was carried out in a modified two-step approach [19]. $IrCl_3 \cdot nH_2O$ was first reacted with an excess of dendritic ligand **LG2** to form a chloride-bridged dimer. Then the dimer was converted to the desired product **G2(pic)** and **G2(acac)**, respectively, by replacing the bridging chloride with picolinic acid or acetylacetone under mild conditions (110 °C). For comparison, the homoleptic

* Corresponding author. Fax: +86 0431 8568 5653.
E-mail address: lixiang@ciac.jl.cn (L. Wang).

0022-328X/$ - see front matter © 2009 Elsevier B.V. All rights reserved.
doi:10.1016/j.jorganchem.2009.03.040

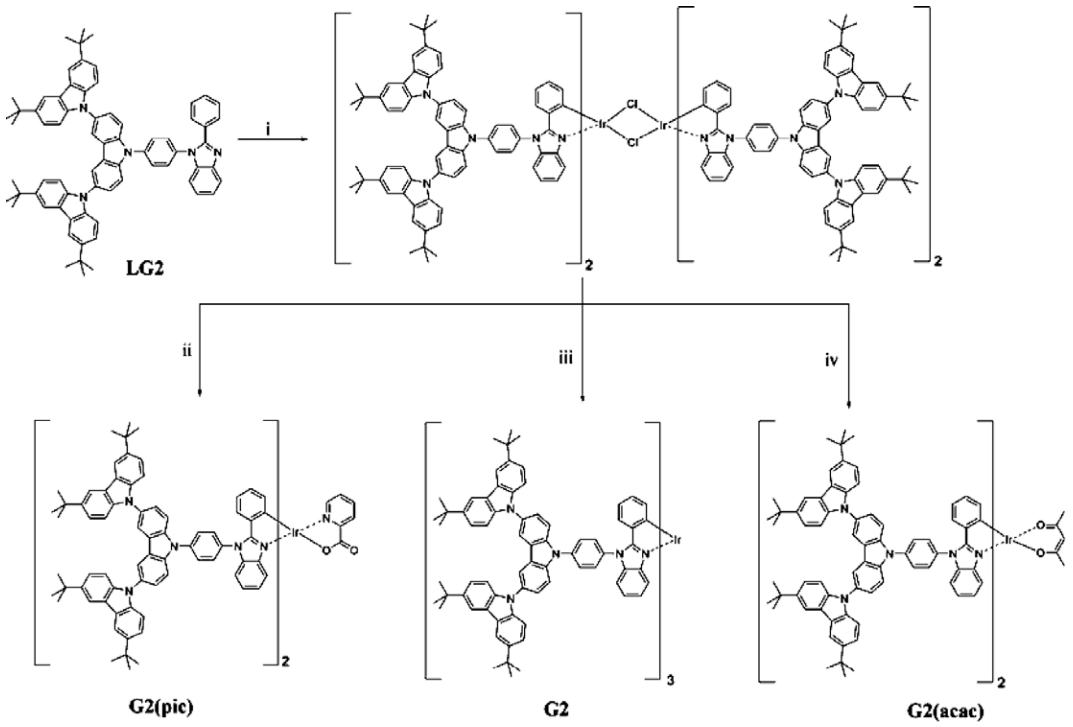

Scheme 1. Synthesis of iridium dendrimers. Reagents and conditions: (i) $IrCl_3{\cdot}nH_2O$, ethoxyethanol, H_2O, THF, reflux; (ii) picolinic acid, ethoxyethanol, chloroform, Na_2CO_3, 110 °C; (iii) K_2CO_3, glycerol, tetraethylene glycol, 230 °C; and (iv) pentane-2,4-dione, ethoxyethanol, chloroform, Na_2CO_3, 110 °C.

dendrimer **G2** was also synthesized according to the literature [7]. The total yields of two steps for **G2(pic)** and **G2(acac)** reached to 55% and 67%, respectively, much higher than that of **G2** (8%), which made it possible to prepare heteroleptic Ir dendrimers with high generation in gram scale. The surface of all the dendrimers was decorated with *tert*-butyl groups to ensure their solubility in common organic solvents. The structures of the dendrimers were verified with ^{1}H NMR, elemental analysis and MALDI-TOF mass spectra.

Fig. 1 shows the absorption spectra in CH_2Cl_2 solutions and the photoluminescence (PL) spectra in toluene of the dendrimers, and their photophysical properties are collected in Table 1. For both the heteroleptic and homoleptic Ir dendrimers, the absorption spectra are similar to each other, except that the intensity around 239 nm corresponding to carbazole units of heteroleptic ones is lower than that of homoleptic ones. All the dendrimers show two major absorption bands. The absorption bands below 360 nm are attributed to spin-allowed ligand-centered (LC) transitions and the weak absorption shoulders in the range of 360–500 nm are assigned to the metal-to-ligand charge-transfer (MLCT) transitions of the Ir complexes.

As seen in Fig. 1, the dendrimer **G2(acac)** in toluene exhibits only a red shift of 4 nm compared with **G2** and its triplet energy level (T_1) estimated from phosphorescence spectra measured at 77 K is the same as that of **G2** (2.43 eV). These facts indicate that replacing the C^N ligand **LG2** with the ancillary ligand acetylacetone does not change the optical properties of the dendrimers obviously. In contrast, with introduction of picolinic acid as an ancillary ligand, the triplet energy of **G2(pic)** increases to 2.53 eV. Correspondingly, the emission peak blue-shifts from 522 nm of **G2** to 511 nm of **G2(pic)** [20]. Similar PL quantum yields (Φ_P) in the range of 0.82–0.89 are observed in Table 1 for all the dendrimers in toluene solutions. From solution to film states, the PL spectra of all the dendrimers have a bathochromic shift, indicating that even for both homoleptic and heteroleptic Ir dendrimers with the second-generation there are still significant intermolecular interactions in the film leading to PL quenching. Interestingly, both **G2(acac)** and **G2** have a decreased bathochromic shift of 9 nm in comparison with **G2(pic)** (17 nm). Furthermore, the lifetimes of **G2(acac)** are close to those of **G2**, albeit a little decrease is found in Table 1.This observations suggest that **G2(acac)** will be a promising candidate used for non-doped devices, similar to **G2**. Therefore, their EL properties with non-doped device configurations are characterized.

As shown in Fig. 2, the non-doped electrophosphorescent devices were fabricated with the configuration of ITO/PEDOT:PSS (50 nm)/Emitting layer/TPBI (60 nm)/LiF (1 nm)/Al (100 nm), in which 1,3,5-tris(2-N-phenylbenzimidazolyl)benzene (TPBI) acted as an electron-transporting and hole-blocking material. The dendrimers alone were used as the emitting layer, by spin-casting a 5 mg/ml chloroform solution at a spin rate of 1200 rpm to form a high quality film of about 30–40 nm thickness.

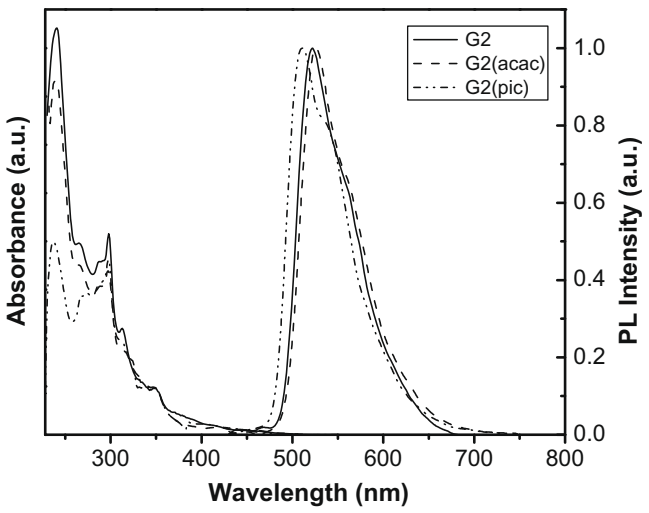

Fig. 1. The absorption spectra in dichloromethane and photoluminescence spectra in toluene at a concentration of 10^{-5} M.

Table 1
Photophysical properties of iridium dendrimers.

	λ_{abs}[a] (log ε) (nm)	λ_{em}[b] (nm)	λ_{em}[c] (nm)	Φ_p[b]	T_1[d] (eV)	τ_1[e] [μs]	τ_2[e] [μs]
G2(pic)	236(5.2), 298(5.2), 408(3.9), 453(3.5)	511	528	0.89	2.53	0.04	0.20
G2	239(5.7), 297(5.3), 414(4.1), 460(3.7)	522	531	0.87	2.43	0.04	0.17
G2(acac)	239(5.4), 297(5.1), 416(3.8), 456(3.5)	526	535	0.82	2.43	0.03	0.15

[a] Measured in CH_2Cl_2 at 298 K with a concentration of 10^{-5} M.
[b] Measured in toluene at 298 K with a concentration of 10^{-5} M and the excitation wavelength of 410 nm.
[c] Neat film data measured at 298 K. PL spectra were measured with the excitation wavelength of 409 nm.
[d] Estimated from the highest energy peak of the phosphorescence spectra at 77 K.
[e] Measured in solid films at 298 K in the air and the lifetimes are obtained by biexponential fit of emission decay curves.

Fig. 3 shows the EL spectra of the dendrimers at a driving voltage of 8 V. Similar to the homoleptic dendrimer **G2**, the heteroleptic dendrimer **G2(acac)** exhibits EL spectrum identical to its PL counterpart with the Commission Internationale de L'Eclairage (CIE) coordinates of (0.40, 0.57), which indicates that the emission is from the triplet excited states of the Ir complexes. However, an additional emission band around 390 nm is observed in the EL spectrum of dendrimer **G2(pic)**, which can be ascribed to the emission of TPBI. Moreover, the intensity of the TPBI emission increases gradually with increasing driving voltages. It is reasonable when their highest occupied molecular orbital (HOMO) energy levels are considered. Owing to the introduction of picolinic acid as the ancillary ligand, the HOMO energy level decreases from −5.02 eV of **G2** to −5.44 eV of **G2(pic)**, improving the hole transportation from the emitting layer/TPBI interface to the inside of TPBI layer and thus leading to the emission of TPBI.

On the other hand, the decreased HOMO energy level for **G2(pic)** would result in the increase of the hole injection barrier. This has been further verified by the high driving voltage as for **G2(pic)**-based non-doped devices. Fig. 4a and b shows the current density–voltage–brightness characteristics and the current density dependence of luminous efficiency of the heteroleptic dendrimers **G2(pic)** and **G2(acac)**, respectively, and the device performance data are tabulated in Table 2. For comparison, **G2** is also characterized at the same conditions. As a result of the increased hole injection barrier, the turn-on voltage increases from 3.5 V of **G2** to 6.7 V of **G2(pic)**. In addition, the driving voltage of **G2(pic)** is much high-

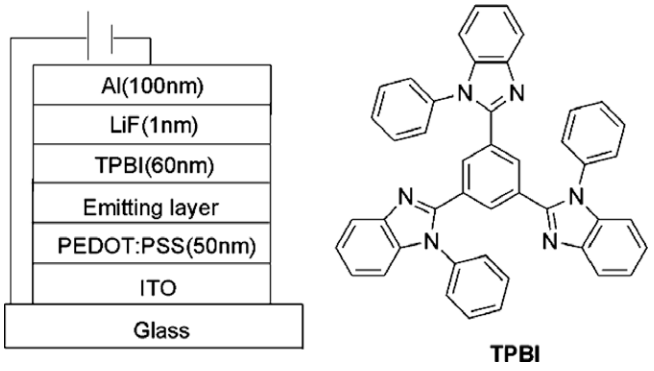

Fig. 2. The device architecture and the chemical structure of the electron transport material in this device.

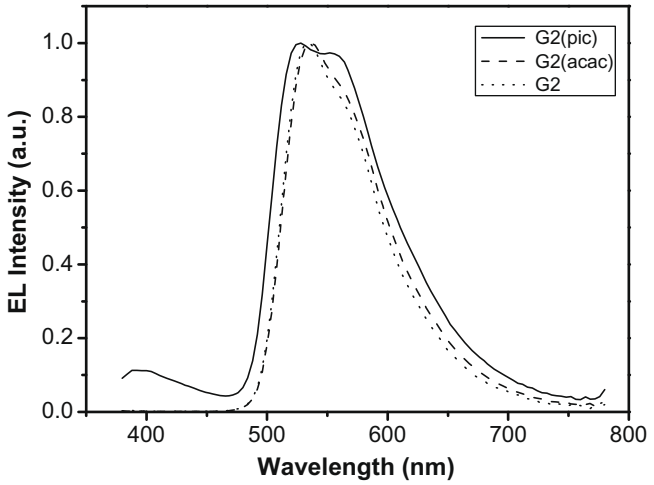

Fig. 3. The electroluminescence spectra of dendrimers at a driving voltage of 8 V.

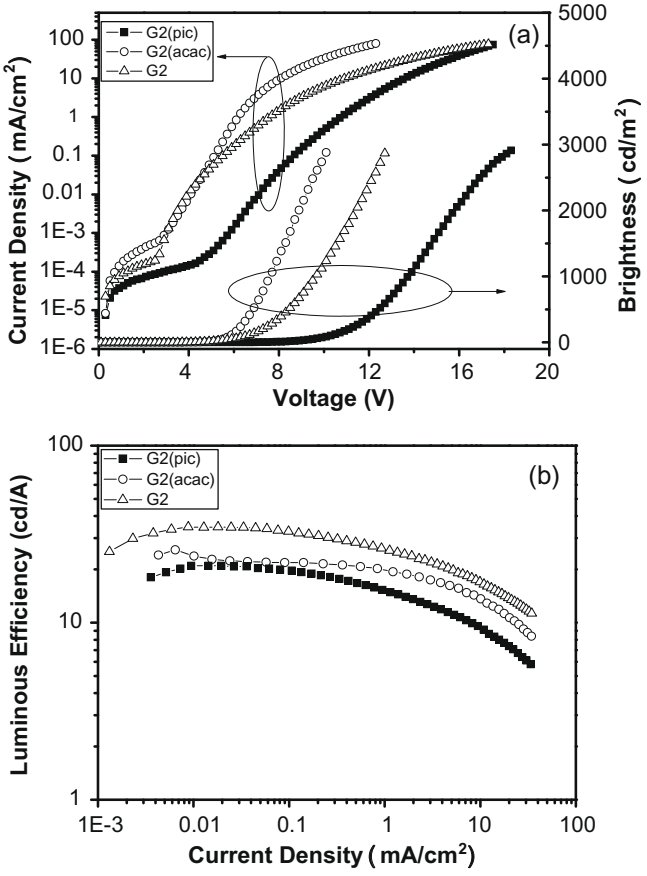

Fig. 4. The current density–voltage–brightness characteristics (a) and the current density dependence of luminous efficiency (b) of the heteroleptic dendrimers **G2(pic)** and **G2(acac)** compared with **G2**.

Table 2
Device properties of iridium dendrimers.

EML	V_{on} (V)	Brightness (cd/m^2)	η_{ext} (%)	η_l (cd/A)	η_p (lm/W)	λ_{max} (nm)	CIE (x, y)
G2(**pic**)	6.7	1000 [a]	3.0	9.0	1.9	528	(0.39,0.54)
		3230 [b]	7.1	21.0	7.9		
G2(**acac**)	3.7	1000 [a]	4.5	15.4	6.3	536	(0.40,0.57)
		4600 [b]	7.7	25.8	20.8		
G2	3.5	1000 [a]	5.9	19.9	6.6	536	(0.40,0.57)
		7840 [b]	10.3	34.7	28.7		

[a] Data at a brightness of 1000 cd/m^2.
[b] The maximum values for brightness, external quantum efficiency (η_{ext}), luminous efficiency (η_l) and power efficiency (η_p).

er than that of **G2** at the same current density or luminance, as can be seen from Fig. 4a.

As shown in Fig. 4b, a maximum external quantum efficiency (EQE) of 7.7% and 7.1%, a maximum luminous efficiency of 25.8 cd/A and 21.0 cd/A, and a maximum brightness of 4600 cd/m^2 and 3230 cd/m^2 for **G2(acac)** and **G2(pic)**, respectively, have been realized. Even at a brightness of 1000 cd/m^2, the efficiencies still remain as high as 4.5% (15.4 cd/A) and 3.0% (9.0 cd/A) for **G2(acac)** and **G2(pic)**, respectively, as illustrated in Table 2. In comparison to **G2**, the EQE of **G2(acac)** at 1000 cd/m^2 only reduces by about 24%. This suggests that **G2(acac)** is also a promising candidate used for non-doped electrophosphorescent devices, especially when the fact that **G2(acac)** can be prepared in a large scale with high yield is taken into account.

3. Conclusion

In conclusion, we have investigated in detail the effect of the ancillary ligands on the synthesis, photophysical properties and device performance of a series of heteroleptic green iridium dendrimers functionalized with carbazole dendrons. Compared with the corresponding homoleptic dendrimers, the heteroleptic dendrimers can be prepared in a gram scale under mild conditions with high yields. Furthermore, these heteroleptic ones possess promising non-doped device performance. For example, dendrimer **G2(acac)** gives a state-of-art peak EQE of 7.7% (25.8 cd/A). Further optimization of the thickness and the morphology of the emitting layer leads to the improved efficiency of 9.8% (33.1 cd/A), together with higher luminance (14 500 cd/m^2). And this work is under way.

4. Experimental

4.1. Synthesis

All chemicals and reagents were used as received from commercial sources without further purification. Solvents for chemical synthesis were purified according to the standard procedures. All chemical reactions were carried out under an inert atmosphere. The dendronized C^N ligand **LG2** and the homoleptic iridium dendrimer **G2** were prepared according to the literature procedures [7].

Chloro-bridged iridium dimer. A mixture of **LG2** (2.2 g, 2.2 mmol), iridium chloride trihydrate (352 mg, 1.0 mmol), 2-ethoxyethanol (30 mL), THF (10 mL) and water (10 mL) was refluxed under argon for 48 h. After cooled to room temperature, the precipitate was collected by filtration and washed with water and ethanol. Then the crude product was purified by column chromatography on silica gel with dichloromethane as eluent to give the chloro-bridged iridium dimer (1.5 g, 69%).

*Heteroleptic dendrimer **G2(pic)***. To the solution of the chloro-bridged iridium dimer (0.57 g, 0.13 mmol) in 2-ethoxyethanol (12 mL) and chloroform (9 mL), picolinic acid (0.07 g, 0.52 mmol), and sodium carbonate (0.14 g, 1.30 mmol) were added. The mixture was stirred at 110 °C for 36 h under argon. After cooling to room temperature, water was added. The mixture was extracted with dichloromethane, washed with water, dried over anhydrous sodium sulfate, and then filtered. After the solvent was removed, the residue was purified by column chromatography on alkaline alumina with dichloromethane–methanol (50:1) as eluent to afford **G2(pic)** (470 mg, 79%). ^{1}H NMR (300 MHz, $CDCl_3$) [ppm]: δ 8.30 (d, J = 7.2 Hz, 1H), 8.25 (s, 4H), 8.19–8.22 (m, 1H), 8.13 (s, 8H), 8.05–8.08 (m, 6H), 7.90–7.93 (m, 4H), 7.78 (d, J = 8.7 Hz, 4H), 7.67 (d, J = 8.8 Hz, 4H), 7.43 (dd, J = 8.7, 1.8 Hz, 10H), 7.32 (dd, J = 8.6, 2.0 Hz, 10H), 7.22–7.23 (m, 2H), 6.89–6.94 (m, 2H), 6.79–6.85 (m, 2H), 6.73–6.76 (m, 2H), 6.66–6.71 (m, 2H), 6.45–6.48 (m, 1H), 5.76 (d, J = 8.7 Hz, 1H), 1.42 (s, 72H). Anal. Calc. for $C_{148}H_{136}N_{11}O_2Ir$: C, 77.52; H, 5.98; N, 6.72. Found: C, 77.34; H, 6.05; N, 6.56%. MALDI-TOF (m/z): 2292.1 [M$^+$], 2170.1 [M$^+$−pic].

*Heteroleptic dendrimer **G2(acac)***. To the solution of the chloro-bridged iridium dimer (0.79 g, 0.18 mmol) in 2-ethoxyethanol (20 mL) and chloroform (10 mL), acetylacetone (0.07 g, 0.72 mmol), and sodium carbonate (0.19 g, 1.80 mmol) were added. The mixture was stirred at 110 °C for 36 h under argon. After cooling to room temperature, water was added. The mixture was extracted with dichloromethane, washed with water, dried over anhydrous sodium sulfate, and then filtered. After the solvent was removed, the residue was purified by column chromatography on alkaline alumina with dichloromethane–petroleum (1:1) as eluent to afford **G2(acac)** (793 mg, 97%). ^{1}H NMR (300 MHz, d_6-DMSO) [ppm]: δ 8.74 (s, 4H), 8.30 (s, 12H), 8.18 (d, J = 8.6 Hz, 2H), 8.08 (d, J = 8.2 Hz, 2H), 7.94 (d, J = 8.6 Hz, 4H), 7.78 (d, J = 8.9 Hz, 4H), 7.66–7.68 (m, 2H), 7.47–7.51 (m, 14H), 7.36 (d, J = 8.6 Hz, 8H), 6.84 (d, J = 7.6 Hz, 2H), 6.69 (t, J = 7.3 Hz, 2H), 6.61 (t, J = 7.4 Hz, 2H), 6.47 (d, J = 7.5 Hz, 2H), 5.35 (s, 1H), 1.86 (s, 6H), 1.42 (s, 72H). Anal. Calc. for $C_{147}H_{139}N_{10}O_2Ir$: C, 77.78; H, 6.17; N, 6.17. Found: C, 77.53; H, 6.13; N, 5.96%. MALDI-TOF (m/z): 2269.2 [M$^+$], 2170.3 [M$^+$−acac].

4.2. Measurement and characterization

^{1}H NMR spectra were recorded with Bruker Avance 300 NMR spectrometer. The elemental analysis was performed using a Bio-Rad elemental analysis system. MALDI/TOF (matrix assisted laser desorption ionization/Time-of-flight) mass spectra were performed on AXIMA CFR MS apparatus (COMPACT). UV–Vis absorption and photoluminescence spectra were measured by Perkin–Elmer Lambda 35 UV/Vis spectrometer and Perkin–Elmer LS 50B spectrofluorometer, respectively. Solution PL quantum efficiency was measured by a relative method using *fac*-Ir(ppy)$_3$ (Φ_p = 0.40 in toluene) as the standard [21]. Phosphorescence spectra at 77 K were measured in a toluene–ethanol–methanol (5:4:1) mixed solvent. The triplet energy of the dendrimers was estimated from the maximum of the first vibronic mode ($S_0^{v=0} \leftarrow T_1^{v=0}$) in phosphorescence spectra at 77 K. The lifetimes of phosphorescence from the samples were measured in the air by exciting the samples with

355 nm light pulses with ca. 3 ns pulse width from a Quanty-Ray DCR-2 pulsed Nd:YAG laser.

4.3. Device fabrication and testing

To fabricate OLEDs, a 50-nm-thick poly(ethylenedioxythiophene):poly(styrene sulfonic acid) (PEDOT:PSS, purchased from H.C. Starck) film was first deposited on the pre-cleaned ITO-glass substrates (100 Ω/square) and then cured at 120 °C in air for 30 min. Then the emitting layer was prepared by spin-coating a chloroform solution of the dendrimer at a concentration of 5 mg/mL. Successively, TPBI, LiF and Al were evaporated at a base pressure less than 10^{-6} Torr (1 Torr = 133.32 Pa) through a shadow mask with an array of 10 mm^2 openings. The electroluminescence (EL) spectra and Commission Internationale de L'Eclairage (CIE) coordinates were measured using a PR650 spectra colorimeter. The current–voltage and brightness–voltage curves of devices were measured using a Keithley 2400/2000 source meter and a calibrated silicon photodiode. All the experiments and measurements were carried out at room temperature under ambient conditions.

Acknowledgements

The authors are grateful to Changchun Institute of Applied Chemistry, Chinese Academy of Sciences (CX07QZJC-24), the National Natural Science Foundation of China (Nos. 20474067, 50673088, 50633040 and 50803062), Science Fund for Creative Research Groups (No. 20621401), and 973 Project (2009CB623601) for financial support of this research.

References

[1] G.R. Newkome, C.N. Moorefield, F. Vögtle, Dendritic Molecules Concept, Synthesis and Perspectives, Wiley–VCH, Weinheim, 1996.
[2] S. Hecht, J.M.J. Fréchet, Angew. Chem., Int. Ed. 40 (2001) 74.
[3] S.-C. Lo, N.A.H. Male, J.P.J. Markham, S.W. Magennis, P.L. Burn, O.V. Salata, I.D.W. Samuel, Adv. Mater. 14 (2002) 975.
[4] J.P.J. Markham, S.-C. Lo, S.W. Magennis, P.L. Burn, I.D.W. Samuel, Phys. Lett. 80 (2002) 2645.
[5] S.-C. Lo, E.B. Namdas, P.L. Burn, I.D.W. Samuel, Macromolecules 36 (2003) 9721.
[6] G. Zhou, W.-Y. Wong, B. Yao, Z. Xie, L. Wang, Angew. Chem. Int. Ed. 46 (2007) 1149.
[7] J. Ding, J. Gao, Y. Cheng, Z. Xie, L. Wang, D. Ma, X. Jing, F. Wang, Adv. Funct. Mater. 16 (2006) 575.
[8] W.-Y. Wong, C.-L. Ho, Coord. Chem. Rev. (2009), doi:10.1016/j.ccr.2009.01.013.
[9] W.-Y. Wong, C.-L. Ho, J. Mater. Chem. (2009), doi:10.1039/b819943d.
[10] W.Y. Wong, C.-L. Ho, Z.-Q. Gao, B.-X. Mi, C.-H. Chen, K.-W. Cheah, Z. Lin, Angew. Chem., Int. Ed. 45 (2006) 7800.
[11] C.-L. Ho, Q. Wang, C.-S. Lam, W.-Y. Wong, D. Ma, L. Wang, Z.-Q. Gao, C.-H. Chen, K.-W. Cheah, Z. Lin, Chem. Asian J. 4 (2009) 89.
[12] C.-L. Ho, W.-Y. Wong, Q. Wang, D. Ma, L. Wang, Z. Lin, Adv. Funct. Mater. 18 (2008) 928.
[13] C.-L. Ho, M.-F. Lin, W.-Y. Wong, W.-K. Wong, C.-H. Chen, Appl. Phys. Lett. 92 (2008) 083301.
[14] C.-L. Ho, W.-Y. Wong, Z.-Q. Gao, C.-H. Chen, K.-W. Cheah, B. Yao, Z. Xie, Q. Wang, D. Ma, L. Wang, X.-M. Xu, H.-S. Kwok, Z. Lin, Adv. Funct. Mater. 18 (2008) 319.
[15] A.B. Tamayo, B.D. Alleyne, P.I. Djurovich, S. Lamansky, I. Tsyba, N.N. Ho, R. Bau, M.E. Thompson, J. Am. Chem. Soc. 125 (2003) 7377.
[16] S. Lamansky, P. Djurovich, D. Murphy, F. Abdel-Razzaq, H.-E. Lee, C. Adachi, P.E. Burrows, S.R. Forrest, M.E. Thompson, J. Am. Chem. Soc. 123 (2001) 4304.
[17] B. Liang, L. Wang, Y. Xu, H. Shi, Y. Cao, Adv. Funct. Mater. 17 (2007) 3580.
[18] J. Ding, J. Lü, Y. Cheng, Z. Xie, L. Wang, X. Jing, F. Wang, Adv. Funct. Mater. 18 (2008) 2754.
[19] J. Ding, J. Gao, Q. Fu, Y. Cheng, D. Ma, L. Wang, Synth. Met. 155 (2005) 539.
[20] C. Adachi, R.C. Kwong, P. Djurovich, V. Adamovich, M.A. Baldo, M.E. Thompson, S.R. Forrest, Appl. Phys. Lett. 79 (2001) 2082.
[21] K.A. King, P.J. Spellane, R.J. Watts, J. Am. Chem. Soc. 107 (1985) 1432.